SCIENTIFIC DATA

microclim: Global estimates of hourly microclimate based on long-term monthly climate averages

Michael R. Kearney[1], Andrew P. Isaac[2] and Warren P. Porter[3]

The mechanistic links between climate and the environmental sensitivities of organisms occur through the microclimatic conditions that organisms experience. Here we present a dataset of gridded hourly estimates of typical microclimatic conditions (air temperature, wind speed, relative humidity, solar radiation, sky radiation and substrate temperatures from the surface to 1 m depth) at high resolution (~15 km) for the globe. The estimates are for the middle day of each month, based on long-term average macroclimates, and include six shade levels and three generic substrates (soil, rock and sand) per pixel. These data are suitable for deriving biophysical estimates of the heat, water and activity budgets of terrestrial organisms.

Design Type(s)	observation design ● data integration
Measurement Type(s)	meteorology
Technology Type(s)	data transformation
Factor Type(s)	
Sample Characteristic(s)	global location ● terrestrial habitat

[1]Department of Zoology, The University of Melbourne, Parkville, VIC 3010, Australia. [2]Victorian Life Sciences Computation Initiative, The University of Melbourne, 187 Grattan St., Carlton, VIC 3010, Australia. [3]Department of Zoology, University of Wisconsin, 250N. Mills St, Madison, WI 53706, USA.
Correspondence and requests for materials should be addressed to M.R.K. (email: mrke@unimelb.edu.au)

Background & Summary

The study of the connections between organisms and climate is a classic question in ecology and has a long history of study[1,2]. It has become one of the dominating topics in ecology in the past 20 years[3–5], in part because of the acknowledgement of the issue of anthropogenic global climate change, but also because of the development of high resolution, gridded climatic datasets for terrestrial environments. The latter technical breakthrough has facilitated the rise of correlative methods for species distribution modelling[3,5,6]. This modelling approach began with the BIOCLIM method[7] (see also Ferrier[8]) and an associated dataset of climatic indices[9] derived from interpolations of weather station observations[10], which are now available on a global scale[11].

Correlative species distribution modelling methods are able to capture statistical relationships between occurrence records and climate, and are powerful tools for defining and projecting climatic envelopes. However, these methods only implicitly capture the processes connecting organisms to climate[12]. An explicit understanding of such processes is not only of great scientific interest, but is also important for applied issues in managing biodiversity under climate change. There is, therefore, rising interest in approaches that can mechanistically connect the functional traits of organisms (e.g., thermal tolerances, desiccation resistance, metabolic processes) to climate[13–15]. Such approaches, however, are constrained by the need to define the actual microclimatic environments experienced by an organism at the appropriate time-scale[16]. The environments experienced will often differ dramatically from those represented by gridded climatic layers, particularly in the terrestrial setting. For example, the air-temperature–based climate layers represent conditions approximately 1.5 m above the ground. In contrast, the body temperature experienced by an organism depends on its height above or below the ground, together with the biophysical interaction of its thermal properties (e.g., size, shape, solar reflectance) with the local air temperature, wind speed, radiation and humidity levels as defined by its habitat (e.g., slope, aspect, shading) (Figure 1). If those conditions are known, potential body temperatures and rates of water exchange can be computed using the principles of biophysical ecology[17–20] and then used to define climatic constraints on the behaviour, distribution and abundance of organisms[15,21–24].

To facilitate such mechanistic studies, here we present a gridded dataset of hourly estimates, for the middle day of each month, of all the microclimatic conditions needed to compute heat and water balances of organisms in terrestrial environments at the global scale (Data Citation 1). This microclimatic dataset, which we have called 'microclim', complements the 'worldclim'[11] (http://www.worldclim.org/) and 'cliMond'[25] (https://www.climond.org/) gridded datasets of macroclimate for correlative species distribution modelling.

Methods

Model description

Microclimatic calculations were made with the microclimate model of the 'Niche Mapper' biophysical modelling package. This model was first described in Porter et al.[20] and Beckman et al.[26], with further descriptions in Porter and Mitchell[27], Fuentes and Porter[28] and Kearney et al.[29] It is a Fortran program that includes routines for hourly calculations of solar and infra-red radiation intensities, above-ground profiles of air temperature, wind velocity and relative humidity, and substrate temperature profiles at ten nodes from the surface down to a user-specified maximum depth (typically around 2 m). These calculations can be made as a function of shading by vegetation, soil properties, thermal properties and terrain (slope, aspect, hill shade). To generate the layers presented in this paper, we used a version of the
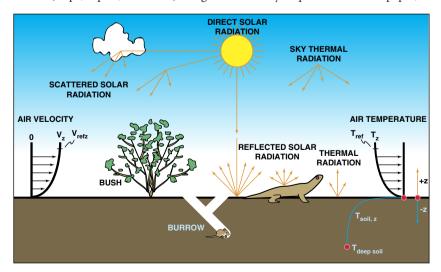

Figure 1. Schematic of microclimatic processes relating to heat and water transfer of an organism, after Porter et al.[20]

Niche Mapper package ('NicheMapR'), which has been set up to run in the R-environment[30] and is being prepared for public release.

The model requires as input the maximum and minimum daily values of air temperature, wind speed, relative humidity and cloud cover, the timing of the maxima and minima relative to dawn or solar noon, soil properties (conductivity, specific heat, density, solar reflectivity, emissivity) as well as the roughness height, slope and aspect. Clear sky solar radiation is computed based on latitude and longitude using the algorithm described in McCullough and Porter[31]. Substrate temperatures are computed based on a one-dimensional partial differential equation that uses above- and below-ground boundary conditions[20]. The substrate surface temperature is computed *via* a heat balance equation, accounting for surface heat exchange *via* radiation, convection, conduction and evaporation. For these simulations we assumed flat ground.

Parameter	Units	Value	Source
Air temperature minimum	—	dawn	Assumed
Air temperature maximum	—	1 h after solar noon	Assumed
Relative humidity minimum	—	1 h after solar noon	Assumed
Relative humidity maximum	—	dawn	Assumed
Wind speed minimum	—	dawn	Assumed
Wind speed maximum	—	1 h after solar noon	Assumed
Cloud cover minimum	—	1 h after solar noon	Assumed
Cloud cover maximum	—	dawn	Assumed
Roughness height of the substrate	m	0.004	Assumed
Substrate longwave infrared emissivity	—	0.96	Assumed
Substrate solar absorptivity	—	0.80	Assumed
Substrate properties: soil			
Soil bulk density	$kg\ m^{-3}$	1400	Assumed
Soil mineral density	$kg\ m^{-3}$	2560	[17]
Soil mineral thermal conductivity	$W\ m^{-1}\ °C^{-1}$	2.5 (0.2 top 5 cm)	[17]
Soil mineral specific heat capacity	$J\ kg^{-1}\ K^{-1}$	870 (1920 top 5 cm)	[17]
Soil saturated water content	$m^3\ m^{-3}$	0.3	[42]
Substrate properties: rock			
Rock bulk density	$kg\ m^{-3}$	2640	Assumed
Rock mineral density	$kg\ m^{-3}$	2640	[17]
Rock mineral thermal conductivity	$W\ m^{-1}\ °C^{-1}$	3.0	[17]
Rock mineral specific heat capacity	$J\ kg^{-1}\ K^{-1}$	820	[17]
Rock saturated water content	$m^3\ m^{-3}$	0	
Substrate properties: sand			
Sand bulk density	$kg\ m^{-3}$	1300	Assumed
Sand mineral density	$kg\ m^{-3}$	2660	[17]
Sand mineral thermal conductivity	$W\ m^{-1}\ °C^{-1}$	8.8	[17]
Sand mineral specific heat capacity	$J\ kg^{-1}\ K^{-1}$	800	[17]
Sand saturated water content	$m^3\ m^{-3}$	0.1	[42]

Table 1. Microclimate model parameters.

Model parameters and input data

For substrate temperature calculations, we used nodes of 0, 2.5, 5, 10, 15, 20, 30, 50, 100 and 200 cm for three different substrate types: soil, rock and sand (see Table 1 for respective substrate parameters). For the 'soil' substrate type, a 5 cm cap of organic material was simulated (see Kearney et al.[29]). The deep substrate temperature (at 200 cm) was assumed to be the mean annual air temperature, based on the monthly daily maximum and minimum air temperatures. All calculations were made for six different levels of shading by vegetation: 0, 25, 50, 75, 90 and 100%. The model produces an hourly output of air temperature, wind speed and relative humidity at the reference height (10 m for wind, 1.2 m for air temperature and relative humidity) and at a second height specified by the user. For the latter we used 1 cm, and report how to interpolate to other heights in the Usage Notes section below.

Climatic data were drawn from a global 10 arc-minute dataset of monthly mean (1961–1990) daily maximum and minimum air temperature and monthly mean daily relative humidity, wind speed and cloud cover[32]. For computations of solar radiation, an aerosol attenuation profile is required[31]. For this we used the 5-degree resolution Global Aerosol Data Set (GADS)[33], modifying the original GADS Fortran program to give output for the full spectral profile for a single location, and using the average of the summer and winter values of aerosol attenuation. For estimates of elevation (from which air pressure was derived for calculating properties of air) we used the 10 arc-minute worldclim grid (http://www.worldclim.org). Monthly soil moisture estimates were obtained from the Climate Prediction Center (NOAA/OAR/ESRL PSD, Boulder, Colorado, USA, http://www.esrl.noaa.gov/psd/). The simulations were run on an IBM iDataplex x86 supercomputer (1120 Intel Sandybridge compute cores running at 2.7 GHz) administered by the Victorian Life Sciences Computation Initiative.

Data Records

The microclim dataset (Data Citation 1) is provided in netCDF format, with one file per variable per month, each file comprising 24 layers (one for each hour of the day from 0:00 h to 23:00 h, so layer 13 is 12:00 midday) for the globe (852 rows, 2159 columns, latitudinal extents −58.57 to 83.43 degrees, longitudinal extents −180.00 to 180.00 degrees). The variables are summarized in Table 2. Shade-specific values are provided for all substrate temperatures as well as for radiant sky temperatures and 1 cm estimates of air temperature and relative humidity. Substrate-specific values are provided for 1 cm air temperature and relative humidity estimates, since they depend on the substrate temperatures.

Variable	Units	Sublevels	Naming convention	Example
Solar zenith angle	degrees	*mon*	ZEN_*mon*.nc	ZEN_1.nc (solar zenith angle for month 1, i.e., January)
Solar radiation	W m^{-2}	*mon*	SOLR_*mon*.nc	SOLR_1.nc (solar radiation for January)
Sky radiant temperature	°C	*mon*, *shd*	TSKY_*shd*_ *mon*.nc	TSKY_25_1.nc (sky radiant temp. for 25% shade, January)
Air temp. at 1.2 m	°C	*mon*	TA120cm_ *mon*.nc	TA120cm_1.nc (air temp. at 120 cm for January)
Air temp. at 1 cm above ground	°C	*mon*, *shd*, *sub*	TA1cm_*sub*_*shd*_*mon*.nc	TA1cm_rock_50_1.nc (air temp. at 1 cm for rock substrate and 50% shade for January)
Wind speed at 10 m	m s^{-1}	*mon*	V10m_*mon*.nc	V10m_1.nc (wind speed at 10 m for January)
Wind speed at 1 cm	m s^{-1}	*mon*	V1cm_*mon*.nc	V1cm_1.nc (wind speed at 1 cm for January)
Relative humidity at 1.2 m	%	*mon*	RH120cm_*mon*.nc	RH120cm_1.nc (relative humidity at 120 cm for January)
Relative humidity at 1 cm	%	*mon*, *shd*, *sub*	RH1cm_*sub*_*shd*_*mon*.nc	RH1cm_sand_100_1.nc (relative humidity at 1 cm for sand substrate and 100% shade for January)
Substrate temp. at specific depths	°C	*mon*, *shd*, *sub*	D*depth*cm_*sub*_*shd*_*mon*.nc	D5cm_rock_75_1.nc (substrate temp. at 5 cm depth for rock substrate and 75% shade for January)

Table 2. The microclim datasets. For the naming convention, the part in italics denotes the particular scenario as follows: *mon* is month of the year (1 to 12, where 1 = Jan, 12 = Dec), *shd* is shade level in % (0, 25, 50, 75, 90, 100), *sub* is substrate (soil, rock, sand).
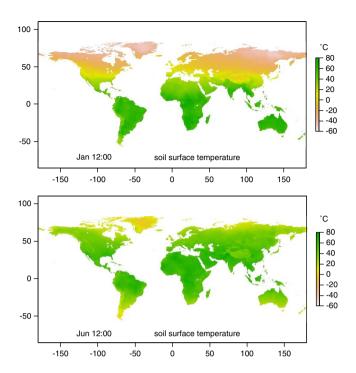
Figure 2. Substrate (soil) surface temperature for 12:00 h in January and June.

Example layers for midday surface temperature in January and June are depicted in Figure 2, and example hourly profiles are provided in Figures 3 and 4, for all variables in January and June for the cool-temperate Australian town of Hobart. Solar zenith angles (Figure 3a and b) are zero when the sun is directly overhead and 90 when it is below the horizon. The solar radiation layers (Figure 3c and d) include the influence of cloud cover as well as the effects of aerosols, with the latter imposing a slightly blocky nature to the layers due to its coarser spatial resolution (5°). The wind speed 1 cm above the ground (Figure 3e and f) is computed from the 10 m reference wind speed based on a standard logarithmic vertical profile and the assumed roughness height (Table 1)[20]. The 1 cm air temperature (Figure 3g and h) is similarly adjusted based on both the 1.2 m reference temperature and the substrate surface temperature, and the 1 cm relative humidity (Figure 3i and j) is temperature-corrected to the 1 cm air temperature based on the relative humidity and air temperature at the 1.2 m reference height (specific humidity is assumed to be homogeneous in the vertical column). Note that our assumption of 'neutral conditions' in the formation of wind speed and air temperature profiles will not be valid for very windy regions of the world, and will result in steeper gradients than would be observed in nature.

The 'sky temperature' (Figure 3g and h) is used to compute the downward longwave radiation flux. All objects emit longwave radiation at a rate proportional to the 4th power of their temperature, $Q_{IR} = \sigma \varepsilon T^4$, where σ is the Stefan Boltzmann constant (W m^{-2} K^{-4}), ε is the emissivity and T is the object's temperature in Kelvin. Clear sky temperature is calculated based on the 1.2 m air temperature using a sky emissivity approximated as $\varepsilon_{SKY} = 1.72(e_A/T_A)^{\frac{1}{7}}$ (equation 10.10 in Campbell and Norman[17]) where T_A is the 1.2 m air temperature in Kelvin and e_A is the vapour pressure of the air in kilopascals. The shade and cloud cover components are calculated assuming an emissivity of 1 and that they are at the 1.2 m air temperature.

Finally, the substrate temperatures at different depths (Figure 4) reflect the influences of the specified soil properties (Table 1) and all the aforementioned variables (day length, radiation levels, wind speeds and air temperature) except relative humidity, as a dry surface was assumed.

Qualitatively, the soil substrate (Figure 4a and b) shows higher amplitude fluctuations near the surface, especially because of the 'organic cap' simulated on top, while the rock substrate (Figure 4e and f) shows greatly dampened fluctuations due to the higher assumed conductivity and heat capacity. The sand shows fluctuations in between those of soil and rock (Figure 4c and d). Note that the 1 cm air temperature, 1 cm relative humidity and substrate temperatures for soil and sand have slightly reduced extent relative to the other layers because of the slightly reduced extent of the soil moisture dataset used in their computation.

In addition, the data record (Data Citation 1) includes model predictions (365-day interpolations) of hourly soil temperature at 177 sites across the USA plotted against 3-hourly observations of soil temperature for all available times between 2011 and 2013 from Soil Climate Analysis Network (SCAN), described in more detail below.
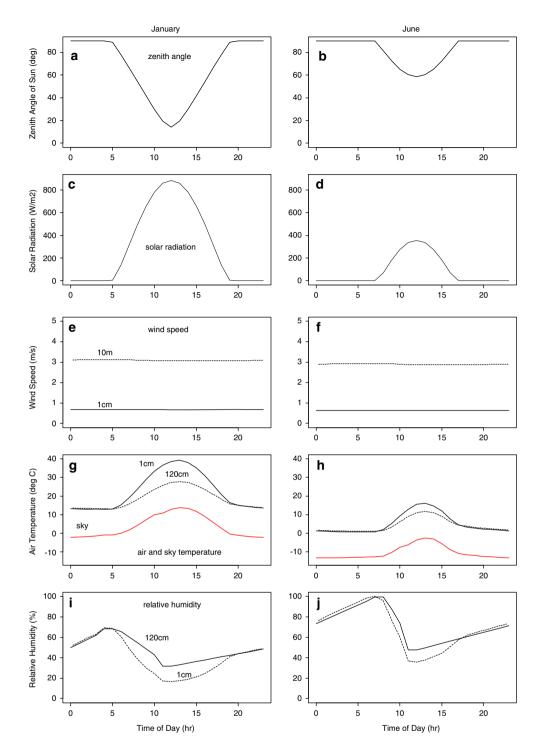
Figure 3. Hourly profiles for January and June for the microclim variables (excluding substrate temperature) for a cool-temperate site—Bushy Parks Estate near Hobart, Tasmania, Australia.

Technical Validation

The microclimate model was recently tested against Australian 3-hourly observations (years 2000–2009) of soil temperature (5, 10, 20, 50 and 100 cm) as well as surface (0.5 cm above the ground) minimum temperature, measured by the Bureau of Meteorology at 43 sites across the continent[29]. The model predicted 85% of the variation in the soil temperature observations with an average accuracy of 2–3.3 °C (~10% of the temperature range at a given depth). For that validation study, historical daily interpolated climatic grids[34] as well as historical monthly soil moisture estimates[35,36] were used as environmental
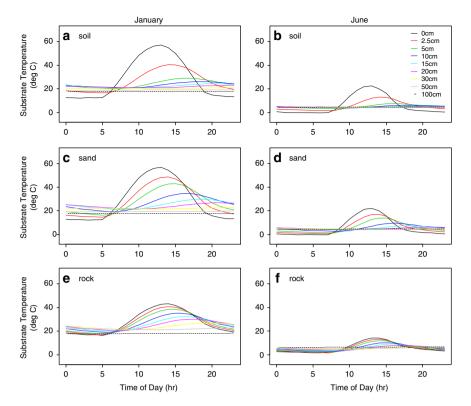
Figure 4. Hourly substrate temperature profiles with depth, for January and June for the microclim variables for a cool-temperate site—Bushy Parks Estate near Hobart, Tasmania, Australia. Examples are shown for the three generic substrate types included in the microclim dataset—soil, sand and rock.

inputs. To compare the performance of the model when driven by the environmental inputs of the present study (i.e., long-term monthly climatic averages), we ran a 3-year simulation based on a daily spline of the monthly inputs ('spline' function of the statistical package 'R' v. 2.15.2 (REF 30)) and compared it to the observations and predictions reported in Kearney et al.[29] for four climatically distinct sites (Supplementary Figures S1–S4). The resulting outputs were extremely similar except that, as expected, more variation was predicted and observed with the daily resolution data at shallow depths. Also, in the original validation study we assumed evaporative cooling on rainy days (see especially the Darwin plots, Supplementary Figure S4), whereas dry ground was always assumed in the present calculations.

In addition to the Australian tests, we have compared the outputs of the model (again, splined across 365 days) for 177 sites across the USA (including Alaska and Puerto Rico) (Supplementary Table S1, see also Supporting Images S1-S177 in the data repository (Data Citation 1)). 3-hourly soil temperature estimates from these sites were extracted from the Soil Climate Analysis Network[37] (SCAN, http://www.wcc.nrcs.usda.gov/scan/), using all available data from 2011–2013. We followed the same procedure as in the Australian tests[29], i.e., we calculated r^2 values for linear regressions of observed vs. predicted temperature as well as the root mean square deviation (RMSD) and proportional root mean square deviation (RMSDp). For these analyses the model predicted 88% of the variation in the soil temperature observations with an accuracy of 3.2–4.5 °C (~13% of the temperature range at a given depth) under the assumption of zero shade. Visual inspection of Supporting Images S1–S177 (which include photos of the stations) indicates clearly where inaccuracies are due to the presence of snow and forest cover.

Usage Notes

The microclim datasets (Data Citation 1) can be used to extract data for specific points or for selected grids, and the user can employ interpolation functions to obtain estimates at finer resolutions of time (i.e., sub-hourly, or daily rather than monthly), shade level and heights above the ground between 1 cm and 120 cm if necessary. Interpolation of wind speed and air temperature between these two heights to any other height z, assuming neutral conditions (i.e., no strong free convection), can be achieved with the

following equations[38]

$$V_z = (V^*/k)\ln(\frac{z}{z_0} + 1)$$

$$\frac{V_z}{V_r} = \frac{T_z - T_s}{T_r - T_s} = \frac{\ln(\frac{z}{z_0} + 1)}{\ln(\frac{z_r}{z_0} + 1)}$$

where V^* is the shear velocity (m s^{-1}), V_z is the wind speed at the new height, V_r is the reference wind speed, z_r is the reference height (m), z_0 is the assumed surface roughness (0.004 m in the present case), T_s is the surface temperature (°C), T_r is the air temperature at the reference height, T_z is the air temperature at the new height, and k is the Karman constant (0.4). In the Supplementary Material we include an R-script (Supplementary Script S1) with examples of how to read the files to memory, plot global grids per hour, and extract and compile a 24 h profile of microclimatic estimates for a particular location.

The monthly-mean character of the macroclimatic data on which these datasets are based must be borne in mind when applying them to ecological problems. Many ecological questions can be answered with microclimatic simulations derived from monthly temporal data resolution (e.g., ref. 39). However, the natural daily variation in surface conditions, especially air temperature, wind gusts and cloud, will impose substantially more variability than implied by these layers. For such applications, the user may impose such variability on the base conditions provided by the microclim layers, e.g., by using environmental bootstraps[40,41] on local air temperature observations. The user should also be aware that we have not simulated snow cover, which will lead to inaccuracies in the soil temperature estimates for snow-covered areas unless otherwise accounted for. If periods of snow cover are known, the microclim layers could be amended for those periods (e.g., by forcing near-surface substrate temperatures to zero).

References

1. Andrewartha, H. G., Birch, L. C. *The Distribution and Abundance of Animals* (The University of Chicago Press, 1954).
2. Woodward, F. I. *Climate and Plant Distribution* (Cambridge University Press, 1987).
3. Elith, J., Leathwick, J. R. Species distribution models: ecological explanation and prediction across space and time. *Annu. Rev. Ecol. Evol. Syst.* **40,** 677–697 (2009).
4. Austin, M. P. Spatial prediction of species distribution: an interface between ecological theory and statistical modelling. *Ecol. Model.* **157,** 101–118 (2002).
5. Guisan, A., Zimmermann, N. E. Predictive habitat distribution models in ecology. *Ecol. Model.* **135,** 147–186 (2000).
6. Guisan, A., Thuiller, W. Predicting species distribution: offering more than simple habitat models. *Ecol. Lett.* **8,** 993–1009 (2005).
7. Nix, H. In *Australian Flora and Fauna Series Number 7: Atlas of Elapid Snakes of Australia* (Australian Government Publishing Service, 1986).
8. Ferrier, S. *The Status of the Rufous Scrub-bird Atrichornis Rufescens: Habitat, Geographical Variation and Abundance* (The University of New England, 1984).
9. *ANUCLIM User Guide v. 5.0* (Centre for Resource and Environmental Studies, Australian National University, Canberra, 2000).
10. Hutchinson, M. F. *Data Assimilation Systems*. BMRC Research Report No. 27 104–113 (Bureau of Meteorology, 1991).
11. Hijmans, R. J., Cameron, S. E., Parra, J. L., Jones, P. G., Jarvis, A. Very high resolution interpolated climate surfaces for global land areas. *Int. J. Climatol.* **25,** 1965–1978 (2005).
12. Dormann, C. F. *et al.* Correlation and process in species distribution models: bridging a dichotomy. *J. Biogeogr.* **39,** 2119–2131 (2012).
13. Kearney, M., Porter, W. P. Mechanistic niche modelling: combining physiological and spatial data to predict species' ranges. *Ecol. Lett.* **12,** 334–350 (2009).
14. Buckley, L. B. *et al.* Can mechanism inform species' distribution models? *Ecol. Lett.* **13,** 1041–1054 (2010).
15. Kearney, M., Simpson, S. J., Raubenheimer, D., Helmuth, B. Modelling the ecological niche from functional traits. *Phil. Trans. R. Soc. B* **365,** 3469–3483 (2010).
16. Geiger, R. *The Climate Near the Ground* (Harvard University Press, 1950).
17. Campbell, G. S., Norman, J. M. *Environmental Biophysics* (Springer, 1998).
18. Gates, D. M. *Biophysical Ecology* (Springer, 1980).
19. Porter, W. P., Gates, D. M. Thermodynamic equilibria of animals with environment. *Ecol. Monogr.* **39,** 227–244 (1969).
20. Porter, W. P., Mitchell, J. W., Beckman, W. A., DeWitt, C. B. Behavioral implications of mechanistic ecology - Thermal and behavioral modeling of desert ectotherms and their microenvironment. *Oecologia* **13,** 1–54 (1973).
21. Buckley, L. B. Linking traits to energetics and population dynamics to predict lizard ranges in changing environments. *Am. Nat.* **171,** E1–E19 (2008).
22. Kearney, M., Porter, W. P. Mapping the fundamental niche: physiology, climate, and the distribution of a nocturnal lizard. *Ecology* **85,** 3119–3131 (2004).
23. Kearney, M. R., Simpson, S. J., Raubenheimer, D., Kooijman, S. A. L. M. Balancing heat, water and nutrients under environmental change: a thermodynamic niche framework. *Funct. Ecol.* **27,** 950–966 (2013).
24. Porter, W. P., Sabo, J. L., Tracy, C. R., Reichman, O. J., Ramankutty, N. Physiology on a landscape scale: plant-animal interactions. *Integr. Comp. Biol.* **42,** 431–453 (2002).
25. Kriticos, D. J. *et al.* CliMond: global high-resolution historical and future scenario climate surfaces for bioclimatic modelling. *Methods in Ecology and Evolution* **3,** 53–64 (2012).
26. Beckman, W. A., Mitchell, J. W., Porter, W. P. Thermal model for prediction of a desert Iguana's daily and seasonal behavior. *J. Heat Transfer* **95,** 257–262 (1973).
27. Porter, W. P., Mitchell, J. W. Method and system for calculating the spatial-temporal effects of climate and other environmental conditions on animals. USA patent 7155377 (2006).
28. Fuentes, M. M. P. B., Porter, W. P. Using a microclimate model to evaluate impacts of climate change on sea turtles. *Ecol. Model* **251,** 150–157 (2013).
29. Kearney, M. R. *et al.* Microclimate modelling at macro scales: a test of a general microclimate model integrated with gridded continental-scale soil and weather data. *Methods in Ecology and Evolution* **5,** 273–286 (2014).

30. R Development Core Team. *R: A language and environment for statistical computing* (R Foundation for Statistical Computing: Vienna, Austria, ISBN 3-900051-07-0, 2012).
31. McCullough, E. C., Porter, W. P. Computing clear day solar radiation spectra for the terrestrial ecological environment. *Ecology* **52,** 1008–1015 (1971).
32. New, M., Lister, D., Hulme, M., Makin, I. A high-resolution data set of surface climate over global land areas. *Climate Res.* **21,** 1–25 (2002).
33. Koepke, P., Hess, M., Schult, I., Shettle, E. P. *Global Aerosol Data Set* (Max-Planck-Institut für Meteorologie: Hamburg, 1997).
34. Jones, D. A., Wang, W., Fawcett, R. High-quality spatial climate data-sets for Australia. *Aust. Meteorol. Oceanogr. J* **58,** 233–248 (2009).
35. Raupach, M. R. *et al. Australian Water Availability Project (AWAP): CSIRO Marine and Atmospheric Research Component*, Final report for Phase 3, 1–67 (Centre for Australian Weather and Climate Research, Bureau of Meteorology and CSIRO: Melbourne, 2009).
36. Raupach, M. R. *et al. CSIRO AWAP Run 26c Historical Monthly and Annual Model Results for 1900-2009* (Centre for Australian Weather and Climate Research, Bureau of Meteorology and CSIRO: Melbourne, 2011).
37. Schaefer, G. L., Cosh, M. H., Jackson, T. J. The USDA Natural Resources Conservation Service Soil Climate Analysis Network (SCAN). *J. Atmos. Oceanic Technol.* **24,** 2073–2077 (2007).
38. Sellers, W. D. *Physical Climatology* (University of Chicago Press, 1965).
39. Kearney, M. R., Matzelle, A., Helmuth, B. Biomechanics meets the ecological niche: the importance of temporal data resolution. *J. Exp. Biol.* **215,** 922–933 (2012).
40. Denny, M. W., Hunt, L. J. H., Harley, C. D. G. On the prediction of extreme ecological events. *Ecol. Monogr.* **79,** 397–421 (2009).
41. Denny, M. W., Dowd, W. W. Biophysics, environmental stochasticity, and the evolution of thermal safety margins in intertidal limpets. *J. Exp. Biol.* **215,** 934–947 (2012).
42. Lambers, H., Chapin, S. F. III, Pons, T. L. *Plant Physiological Ecology* (Springer, 2008).

Data Citation

1. Kearney, M. R., Isaac, A. P., Porter, W. P. Figshare, http://dx.doi.org/10.6084/m9.figshare.878253 (2014).

Acknowledgements

Author Contributions

M.R.K designed the study, wrote the MS and contributed to model development, M.R.K and A.P.I computed the data layers, W.P.P developed the microclimate model.

Additional information

Supplementary information accompanies this paper at http://www.nature.com/sdata.

Competing financial interests: The authors declare no competing financial interests.

How to cite this article: Kearney, M. R. *et al.* microclim: Global estimates of hourly microclimate based on long-term monthly climate averages. *Sci. Data* 1:140006 doi: 10.1038/sdata.2014.6 (2014).